Anti-Cancer Drugs 1999, **10**, pp. 685–692

Preclinical study

Synthesis of [^{99m}Tc]ethylenedicysteine–colchicine for evaluation of antiangiogenic effect

Fereshteh Zareneyrizi, David J Yang, Chang-Sok Oh, Seyfettin Ilgan, Dong-Fang Yu, Wayne Tansey, Chun-Wei Liu, E Edmund Kim and Donald A Podoloff
Divisions of Diagnostic Imaging, University of Texas MD Anderson Cancer Center, Houston, TX 77030, USA.

Angiogenesis is in part responsible for tumor growth and the development of metastasis. Radiolabeled angiongenesis inhibitors would be useful to assess tumor microvasculature density. Colchicine (COL), a potent antiangiogenic agent, is known to inhibit microtubule polymerization and cell arrest at metaphase. This study aimed to develop ^{99m}Tc-labeled COL (EC-COL) using ethylenedicysteine (EC) as a chelator to assess tumor microvascular density. EC was conjugated to trimethylcolchicinic acid using *N*-hydroxysuccinimide and 1-ethyl-3-dimethylaminopropyl carbodiimide as coupling agents with a yield of 50–60%. *In vivo* stability was analyzed in rabbit serum at 0.5–4 h. Tissue distribution and planar imaging studies of [^{99m}Tc]EC-COL were evaluated in breast tumor-bearing rats at 0.5, 2 and 4 h. The data was compared to that using [^{99m}Tc]EC (control). The radiochemical yield of [^{99m}Tc]EC-COL was greater than 95%. [^{99m}Tc]EC-COL was stable in rabbit serum. *In vivo* biodistribution of [^{99m}Tc]EC-COL in breast tumor-bearing rats showed increased tumor-to-blood (0.52 ± 0.12 to 0.72 ± 0.07) and tumor-to-muscle (3.47 ± 0.40 to 7.97 ± 0.93) ratios as a function of time. Conversely, tumor-to-blood values showed a time-dependent decrease with [^{99m}Tc]EC over the same time period. Planar images confirmed that the tumors could be visualized clearly with [^{99m}Tc]EC-COL from 0.5 to 4 h. [^{99m}Tc]EC-COL may be useful to assess antiangiogenic and therapeutic effects during chemotherapy. [© 1999 Lippincott Williams & Wilkins.]

Key words: Antiangiogenesis, colchicine, [^{99m}Tc]ethylenedicysteine, tumor imaging.

Introduction

Angiogenesis is in part responsible for tumor growth and the development of metastasis. Antimitotic compounds are antiangiogenic and are known for their potential use as anticancer drugs. These compounds inhibit cell division during the mitotic phase of the cell cycle. Microtubules are involved during the biochemical process of cellular functions, such as cell division, cell motility, secretion, ciliary and flagellar movement, intracellular transport, and the maintenance of cell shape. It is known that antimitotic compounds bind with high affinity to microtubule proteins (tubulin), disrupting microtubule assembly and causing mitotic arrest of the proliferating cells. Thus, antimitotic compounds are considered as microtubule inhibitors or as spindle poisons.[1]

Many classes of antimitotic compounds control microtubule assembly-disassembly by binding to tubulin. Compounds such as colchicinoids interact with tubulin on the colchicine (COL) binding sites and inhibit microtubule assembly.[2,3] Among colchicinoids, COL is an effective anti-inflammatory drug used to treat prophylaxis of acute gout. COL is also used in chronic myelocytic leukemia. Although colchicinoids are potent against certain types of tumor growth, the clinical therapeutic potential is limited due to inability to separate the therapeutic and toxic effects.[1] However, COL may be useful as a biochemical tool to assess cellular functions. Therefore, we developed a radiolabeled COL for the assessment of biochemical process on tubulin functions.

Due to favorable physical characteristics as well as extremely low price, ^{99m}Tc have been preferred to label radiopharmaceuticals. Several compounds have been labeled with ^{99m}Tc using nitrogen and sulfur chelates.[4–7] Bis-aminoethanethiol tetradentate ligands, also called diaminodithiol compounds, are known to form very stable Tc(V)O complexes on the basis of efficient binding of the oxotechnetium group to two thiolsulfur and two amine nitrogen atoms. ^{99m}Tc-L,L-ethylenedicysteine ([^{99m}Tc]EC) is a recent and successful example of N_2S_2 chelates. EC can be labeled

Correspondence to DJ Yang, Department of Nuclear Medicine, University of Texas MD Anderson Cancer Center, 1515 Holcombe Boulevard, Houston, TX 77030, USA.
Tel: (+1) 713 745-3368; Fax: (+1) 713 794-5456;
E-mail: dyang@rpisun1.mdacc.tmc.edu

with ^{99m}Tc easily and efficiently with high radiochemical purity and stability, and is excreted through the kidney by active tubular transport.[8,9]

In this report, synthesis and breast tumor imaging potential using a new [^{99m}Tc]EC-COL were evaluated.

Materials and methods

The nuclear magnetic resonance (NMR) and mass spectral analysis were conducted at the University of Texas Health Science Center (Houston, TX). NMR spectra were recorded on a Bruker 200 MHz Spectrometer. The mass data were obtained by fast atom bombardment on a Kratos MS 50 instrument (England). Sulfo-*N*-hydroxysuccinimide (Sulfo-NHS) and 1-ethyl-3-(3-dimethylaminopropyl) carbodiimide-HCl (EDC) were purchased from Pierce (Radford, IL). All other chemicals were purchased from Aldrich (Milwaukee, WI). Silica gel coated thin-layer chromatography (TLC) plates were purchased from Whatman (Clifton, NJ). ^{99m}Tc-pertechnetate was obtained from a commercial ^{99}Mo/^{99m}Tc generator (Ultratechnekow FM; Mallinckrodt Diagnostica, Holland).

Synthesis of L,L-ethylenedicysteine (EC)

EC was prepared in a two-step synthesis according to the previously described methods.[4,5] The precursor, L-thiazolidine-4-carboxylic acid, was synthesized (m.p. 195°C, reported 196–197°C). EC was then prepared (m.p. 237°C, reported 251–253°C). The structure was confirmed by ^{1}H-NMR and mass spectroscopy (FAB-MS) *m/z* 268 (M^+, 100).

Synthesis of (amino analog of COL) COL-NH_2

The demethylated amino and hydroxy analog of COL was synthesized according to the previously described methods.[10] Briefly, COL (4 g) was dissolved in 100 ml of water containing 25% sulfuric acid. The reaction mixture was heated for 5 h at 100°C. The mixture was neutralized with sodium carbonate. The product was filtered and dried over a freeze dryer, and yielded 2.4 g (70%) of the desired amino analog (m.p. 153–155°C, reported 155–157°C). Ninhydrin (2% in methanol) spray indicated the positivity of the amino group of COL-NH_4. The structure was confirmed by ^{1}H-NMR and mass spectroscopy (FAB-MS). ^{1}H-NMR ($CDCl_3$) δ 8.09 (S, 1H), 7.51 (d, 1H, J=12 Hz), 7.30 (d, 1H, J=12 Hz), 6.56 (S, 1H), 3.91 (S, 6H), 3.85 (m, 1H), 3.67 (S, 3H), 2.25–2.52 (m, 4H). *m/z* 308.2(M^+, 20), 307.2 (100).

Synthesis of EC-COL

Sodium hydroxide (2 N, 0.2 ml) was added to a stirred solution of EC (134 mg, 0.50 mmol) in water (5 ml). To this colorless solution, sulfo-NHS (217 mg, 1.0 mmol) and EDC (192 mg, 1.0 mmol) were added. COL-NH_2 (340 mg, 2.0 mmol) was then added. The mixture was stirred at room temperature for 24 h. The mixture was dialyzed for 48 h using a Spectra/POR molecular porous membrane with cut-off at 500 (Spectrum Medical Industries, Houston, TX). After dialysis, the product was frozen dried using a lyophihlizer (Labconco, Kansas City, MO). The product weighed 315 mg (yield 55%). ^{1}H-NMR (D_2O) δ 7.39 (S, 1H), 7.20 (d, 1H, J=12 Hz), 7.03 (d, 1H, J=12 Hz), 6.78 (S, 1H), 4.25–4.40 (m, 1H), 3.87 (S, 3H,-OCH_3), 3.84 (S, 3H,-OCH_3), 3.53 (S, 3H,-OCH_3), 3.42–3.52 (m, 2H), 3.05–3.26 (m, 4H), 2.63–2.82 (m, 4H), 2.19–2.25 (m, 4H). FAB MS *m/z* 580 (sodium salt, 20). The synthetic scheme of EC-COL is shown in Figure 1.

Radiolabeling of EC-COL and EC with ^{99m}Tc

Radiosynthesis of [^{99m}Tc]EC-COL was achieved by adding the required amount of ^{99m}Tc-pertechnetate into a home-made kit containing the lyophilized residue of EC-COL (5 mg), $SnCl_2$ (100 μg), Na_2HPO_4 (13.5 mg), ascorbic acid (0.5 mg) and NaEDTA (0.5 mg). The final pH of the preparation was 7.4. [^{99m}Tc]EC was also obtained by using a home-made kit containing the lyophilized residue of EC (5 mg), $SnCl_2$ (100 μg), Na_2HPO_4 (13.5 mg), ascorbic acid (0.5 mg) and NaEDTA (0.5 mg) at pH 10. The final pH of the preparation was then adjusted to 7.4. Radiochemical purity was determined by TLC (ITLC SG; Gelman Sciences, Ann Arbor, MI) eluted with ammonium acetate (1 M) in water:methanol (4:1). Radio-TLC (Bioscan, Washington, DC) was used to analyze the radiochemical purity for both radiotracers.

Stability of assay of [^{99m}Tc]EC-COL

The stability of labeled [^{99m}Tc]EC-COL was tested in serum samples. Briefly, 740 kBq of 5 mg [^{99m}Tc]EC-

COL was incubated in the rabbit serum (500 μl) at 37°C for 4 h. The serum samples were diluted with 50% methanol in water, and radio-TLC repeated at 0.5, 2 and 4 h as described above.

Tissue distribution studies

The animal experiments were approved by The University of Texas MD Anderson Institutional Animal

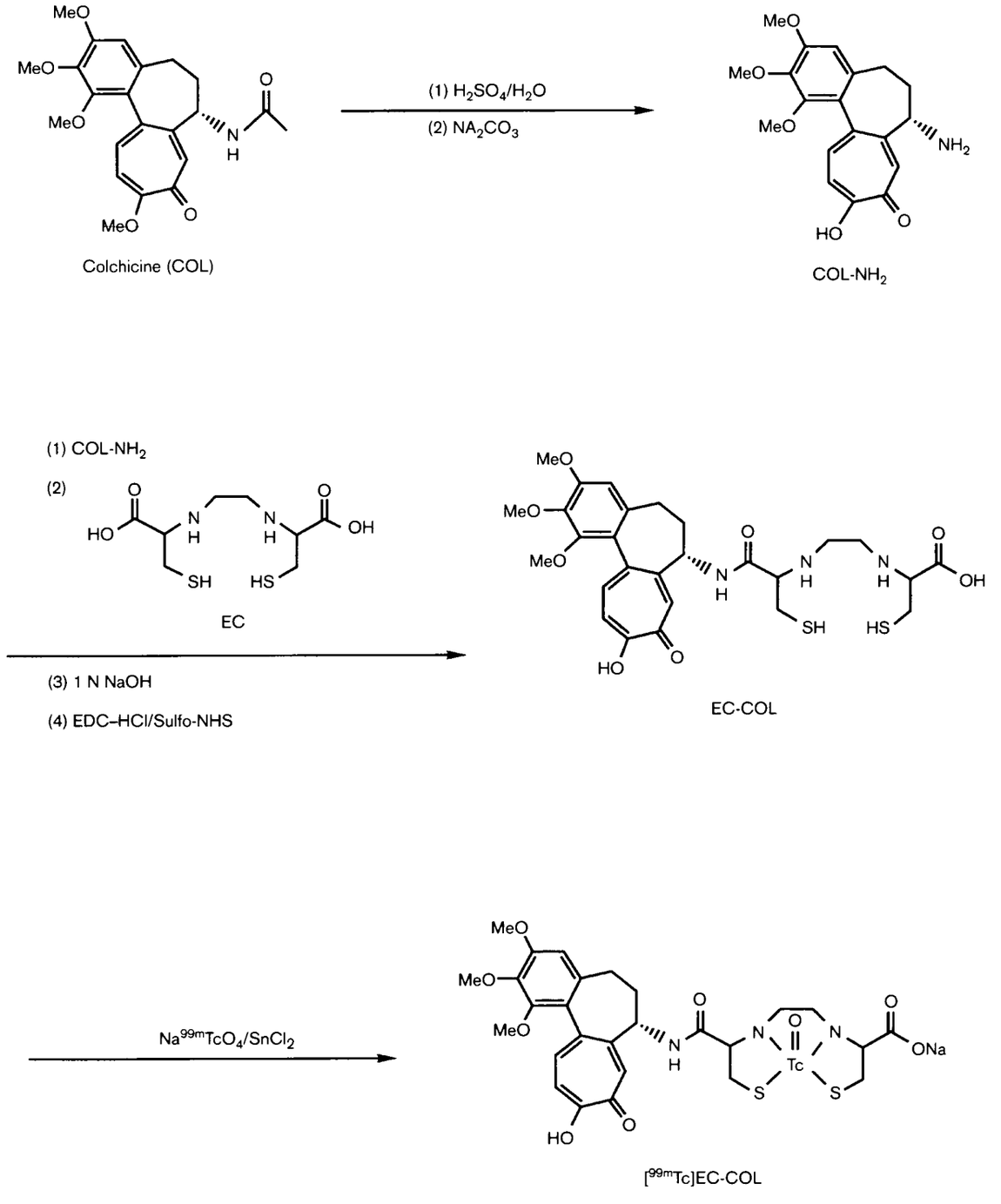

Figure 1. Synthetic scheme of [^{99m}Tc]EC-COL.

Care and Use Committee (IACUC). Female Fischer 344 rats (150 ± 25 g) (Harlan Sprague-Dawley, Indianapolis, IN) were inoculated s.c. with 0.1 ml of mammary tumor cells from the 13762 tumor cell line suspension (10^6 cells/rat, a tumor cell line specific to Fischer rats) into the hind legs using 25-gauge needles. Studies were performed 14–17 days after implantation when tumors reached approximately 1 cm diameter. Rats were anesthetized with ketamine (10–15 mg/rat, i.p.) before each procedure.

In tissue distribution studies, each animal was injected i.v. with 370–550 KBq of [^{99m}Tc]EC-COL or [^{99m}Tc]EC (n=3/time point). The injected mass of [^{99m}Tc]EC-COL was 10 μg per rat. At 0.5, 2 and 4 h following administration of the radiotracers, the rats were sacrificed, and the selected tissues were excised, weighed and counted for radioactivity. The biodistribution of tracer in each sample was calculated as percentage of the injected dose per gram of tissue wet weight (%ID/g). Tumor/non-target tissue count density ratios were calculated from the corresponding %ID/g values. Student's t-test was used to assess the significance of differences between groups.

Scintigraphic imaging studies

Scintigraphic images, using a γ-camera (Siemens Medical Systems, Hoffman Estates, IL) equipped with a low-energy, parallel-hole collimator, were obtained 0.5, 2 and 4 h after i.v. injection of 300 μCi of [^{99m}Tc]EC-COL and [^{99m}Tc]EC. A computer outlined region of interest (ROI) was used to quantitate (counts per pixel) the tumor uptake versus normal muscle uptake.

Results

Radiosynthesis and stability of [^{99m}Tc]EC-COL

Radiosynthesis of EC-COL with ^{99m}Tc was achieved with high (>95%) radiochemical purity (Figure 2). [^{99m}Tc]EC-COL was found to be stable at 0.5, 2 and 4 h in rabbit serum samples. No degradation products were observed.

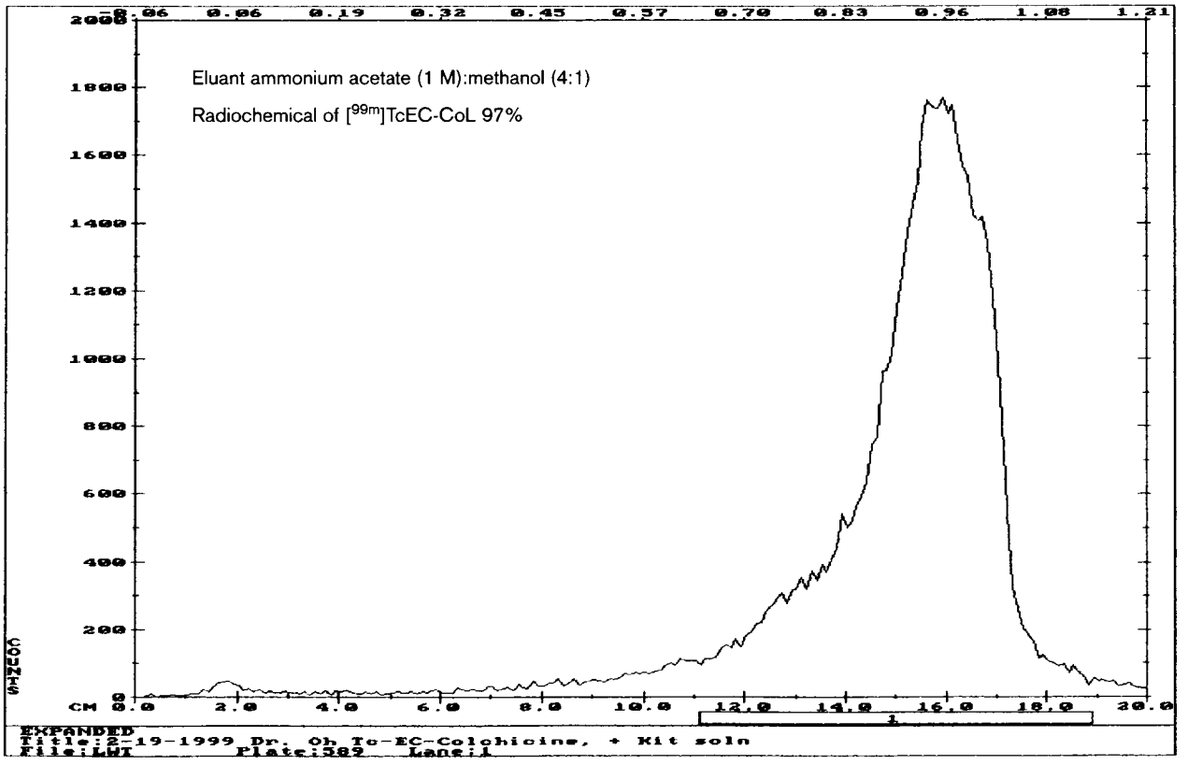

Figure 2. Radio-TLC of [^{99m}Tc]EC-COL.

In vivo biodistribution

The *in vivo* biodistribution of [^{99m}Tc]EC-COL and [^{99m}Tc]EC in breast tumor bearing rats is shown in Tables 1 and 2. Tumor uptake values (%ID/g) of [^{99m}Tc]EC-COL at 0.5, 2 and 4 h was 0.436±0.089, 0.395±0.154 and 0.221±0.006 (Table 1), whereas those for [^{99m}Tc]EC were 0.342±0.163, 0.115±0.002

Table 1. Biodistribution of [^{99m}Tc]EC-COL in breast tumor bearing rats[a]

	30 min	2 h	4 h
Blood	0.837±0.072	0.606±0.266	0.307±0.022
Lung	0.636±0.056	0.407±0.151	0.194±0.009
Liver	1.159±0.095	1.051±0.213	0.808±0.084
Spleen	0.524±0.086	0.559±0.143	0.358±0.032
Kidney	9.705±0.608	14.065±4.007	11.097±0.108
Muscle	0.129±0.040	0.071±0.032	0.028±0.004
Stomach	0.484±0.386	0.342±0.150	0.171±0.123
Uterus	0.502±0.326	0.343±0.370	0.133±0.014
Thyroid	3.907±0.997	2.297±0.711	1.709±0.776
Tumor	0.436±0.089	0.395±0.154	0.221±0.006

[a]Each rat received [^{99m}Tc]EC-COL (10 μCi, i.v.). Each value is the percent of injected dose per gram tissue weight (n=3)/time interval. Each data represents mean of three measurements with SD.

Table 2. Biodistribution of [^{99m}Tc]EC in breast tumor bearing rats[a]

	30 min	2 h	4 h
Blood	0.435±0.029	0.211±0.001	0.149±0.008
Lung	0.272±0.019	0.144±0.002	0.120±0.012
Liver	0.508±0.063	0.286±0.073	0.234±0.016
Spleen	0.118±0.008	0.075±0.002	0.067±0.003
Kidney	7.914±0.000	9.116±0.053	7.834±1.018
Muscle	0.060±0.006	0.028±0.009	0.019±0.001
Stomach	0.136±0.060	0.038±0.027	0.043±0.001
Uterus	0.218±0.036	0.076±0.000	0.074±0.020
Thyroid	0.219±0.036	0.106±0.003	0.083±0.005
Tumor	0.342±0.163	0.115±0.002	0.097±0.005

[a]Each rat received [^{99m}Tc]EC (10 μCi, i.v.). Each value is the percent of injected dose per gram tissue weight (n=3)/time interval. Each data represents mean of three measurements with SD.

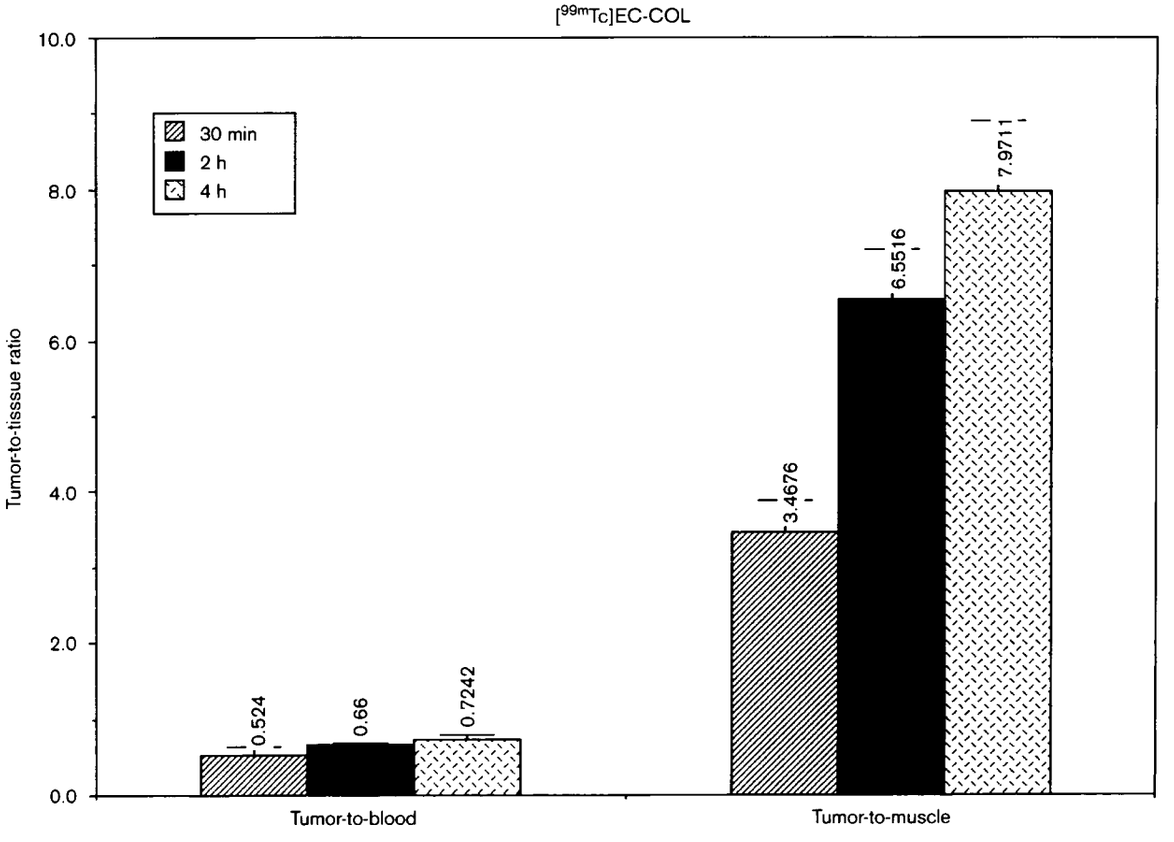

Figure 3. Tumor-to-blood and tumor-to-muscle count density ratios of [^{99m}Tc]EC-COL in breast tumor bearing rats as a function of time. Data are expressed as the mean±SE for n=3 rats per group.

and 0.097 ± 0.005, respectively (Table 2). Increased tumor-to-blood (0.52 ± 0.12 to 0.72 ± 0.07) and tumor-to-muscle (3.47 ± 0.40 to 7.97 ± 0.93) ratios as a function of time were observed in [^{99m}Tc]EC-COL group (Figure 3). Conversely, tumor-to-blood and tumor-to-muscle values showed a time-dependent decrease with [^{99m}Tc]EC when compared to the [^{99m}Tc]EC-COL group over the same time period (Figure 4).

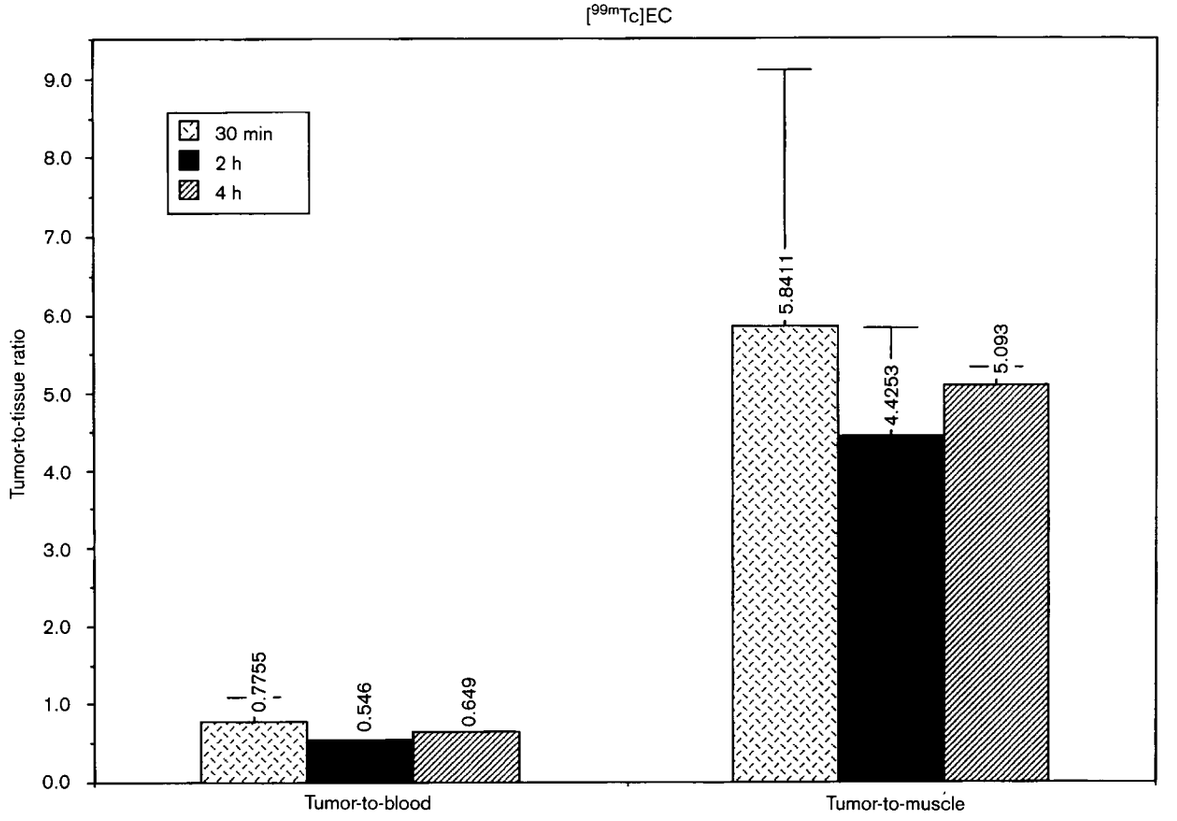

Figure 4. Tumor-to-blood and tumor-to-muscle count density ratios of [^{99m}Tc]EC in breast tumor bearing rats as a function of time. Data are expressed as the mean $\pm$ SE for n=3 rats per group.

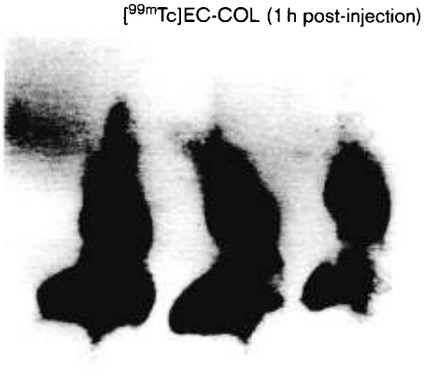

Figure 5. Anterior view of breast tumor bearing rats receiving [^{99m}Tc]EC-COL (300 μCi, i.v.) showed that there was tumor uptake at 1 h post-injection.

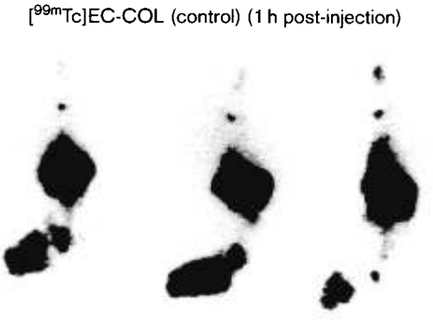

Figure 6. Anterior view of breast tumor bearing rats receiving [^{99m}Tc]EC (300 μCi, i.v.) showed that there was less tumor uptake at 1 h post-injection compared to [^{99m}Tc]EC-COL.

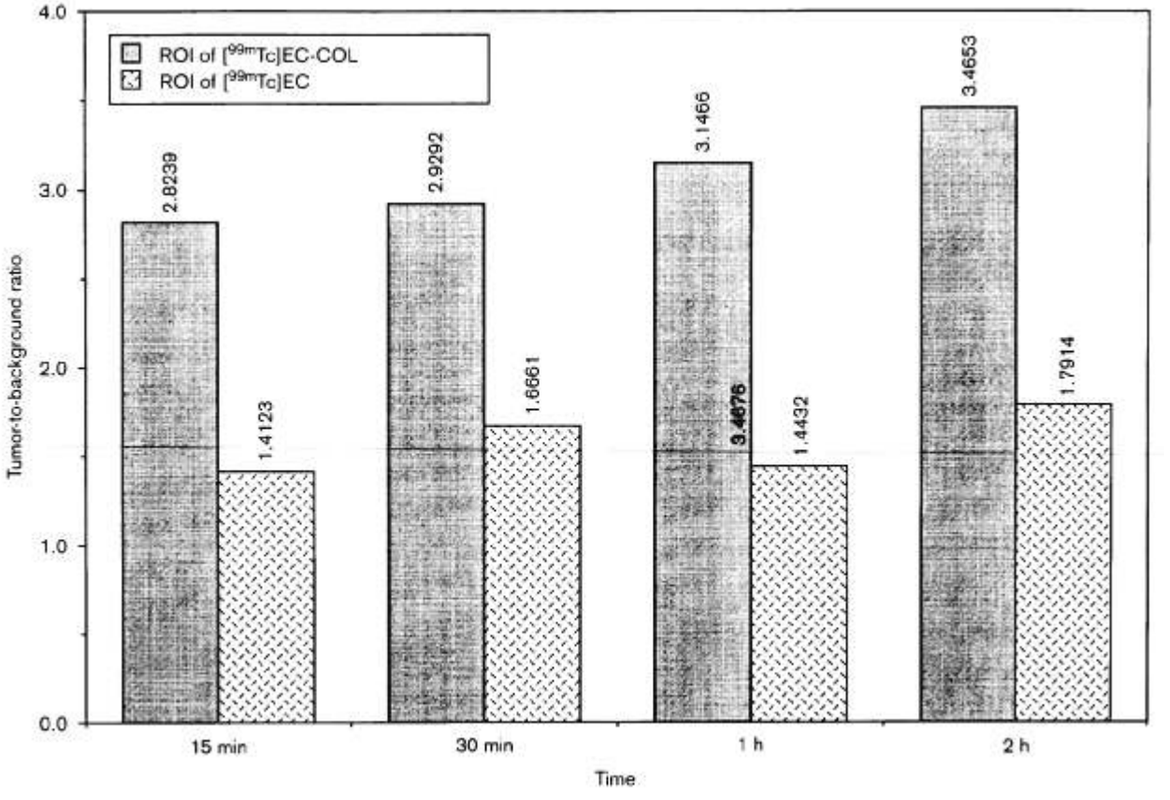

Figure 7. Computer outlined ROI comparison of tumor-to-background ratios between [^{99m}Tc]EC-COL and [^{99m}Tc]EC in breast tumor bearing rats.

Gamma scintigraphic imaging of [^{99m}Tc]EC-COL in breast tumor bearing rats

In vivo imaging studies in three breast tumor bearing rats at 1 h post-administration indicated that the tumor could be visualized well with the [^{99m}Tc]EC-COL group (Figure 5), whereas less tumor uptake in the [^{99m}Tc]EC group was observed (Figure 6). The computer outlined ROI showed that tumor/background ratios in the [^{99m}Tc]EC-COL group were significantly higher than the [^{99m}Tc]EC group (Figure 7).

Discussion

Due to better imaging characteristics and lower price, attempts are made to replace the ^{123}I-, ^{131}I-, ^{67}Ga- and ^{111}In-labeled compounds with corresponding ^{99m}Tc-labeled compounds when possible. Verbruggen *et al.* reported that EC can be labeled with ^{99m}Tc very easily and efficiently at room temperature with high radiochemical purity, and the preparation remains stable for at least 8 h.[7] Because of the reported labeling capacity and rapid renal clearance, EC was selected to synthesize a new ^{99m}Tc-labeled COL. EC-COL was prepared using a relatively simple and fast chemistry. A labeling kit was also developed. Radio-TLC results with the [^{99m}Tc]EC-COL kit confirm the high radiochemical purity and stability in serum.

In the tissue distribution studies, although no significance difference of tumor-to-blood uptake between [^{99m}Tc]EC-COL and [^{99m}Tc]EC groups was observed, there was a significantly increased tumor-to-tissue uptake ratio as a function of time within the [^{99m}Tc]EC-COL group. Planar imaging of [^{99m}Tc]EC-COL demonstrated the feasibility to image tumors at 1 h post-injection.

The development of new ligands to assess the anti-tubulin effect is clinically desirable for the assessment of treatment outcome. Microtubules are involved in the biochemical process of cellular functions. Microtubulin is associated with cell mitosis and angiogen-

esis. Antimitotic compounds such as vincristine and COL bind with high affinity to microtubule proteins (tubulin), disrupting microtubule assembly and causing mitotic arrest of the proliferating cells. In addition to disrupted microtubule depolymerization, COL also induced apoptotic cell death.[11-18] Apoptosis (programmed cell death) occurs during the treatment of cancer with chemotherapy and radiation. Assessment of apoptosis would be useful to evaluate the efficacy of therapy such as disease progression or regression.

In summary, this study demonstrates the feasibility of using [^{99m}Tc]EC-COL for *in vivo* imaging of breast tumors. The findings support further studies on determining treatment outcome by monitoring disease progression using [^{99m}Tc]EC-COL and correlating histopathological findings associated with apoptosis.

Acknowledgments

The authors wish to thank Dianne Perez for her secretarial support. This work was supported in part by the John S Dunn Foundation and Pioneer Pharmaceutical Research Fund.

References

1. Lu MC. Antimotitic agents. In: Foye WO, ed. *Cancer chemotherapeutic agents*. Washington, DC: American Chemical Society 1995: 345-68.
2. Goh EL, Pircher TJ, Lobie PE. Growth hormone promotion of tubulin polymerization stabilizes the microtubule network and protects against colchicine-induced apoptosis. *Endocrinology* 1998; **139**: 4364-72.
3. Wang TH, Wang HS, Ichijo H, *et al.* Microtubule-interfering agents activate c-Jun N-terminal kinase/stress-activated protein kinase through both Ras and apoptosis signal-regulating kinase pathways. *J Biol Chem* 1998; **273**: 4928-36.
4. Ratner S, Clarke HT. The action of formaldehyde upon cysteine. *J Am Chem Soc* 1937; **59**: 200-6.
5. Blondeau P, Berse C, Gravel D. Dimerization of an intermediate during the sodium in liquid ammonia reduction of L-thiazolidine-4-carboxylic acid. *Can J Chem* 1967; **45**: 49-52.
6. Davison A, Jones AG, Orvig C, Sohn M. A new class of oxotechnetium(+5) chelate complexes containing a $TcON_2S_2$ core. *Inorg Chem* 1981; **20**: 1629-32.
7. Verbruggen AM, Nosco DL, Van Nerom CG, *et al.* Tc-99m-L,L-ethylenedicysteine: a renal imaging agent. I. Labelling and evaluation in animals. *J Nucl Med* 1992; **33**: 551-7.
8. Van Nerom CG, Bormans GM, De Roo MJ, Verbruggen AM. First experience in healthy volunteers with Tc-99m-L,L-ethylenedicysteine, a new renal imaging agent. *Eur J Nucl Med* 1993; **20**: 783-46.
9. Surma MJ, Wiewiora J, Liniecki J. Usefulness of Tc-99m-*N,N'*-ethylene-1-dicysteine complex for dynamic kidney investigations. *Nucl Med Commun* 1994; **15**: 628-35.
10. Raffauf RF, Farren AL, Ullyot GE. Colchicine. Derivatives of trimethylcolchicinic acid. *J Am Chem Soc* 1953; **75**: 5292-4.
11. Suzuki Y, Takeda M, Obara N, Suzuki N. Colchicine-induced cell death and proliferation in the olfactory epithelium and vomeronasal organ of the mouse. *Anat Embryol* 1998; **198**: 43-51.
12. Ceccatelli S, Ahlborn E, Diana A, Zhivotocsky B. Apoptosis in rat hippocampal dentate gyrus after intraventricular colchicine. *Neuroreport* 1997; **8**: 3779-83.
13. Bumbasirevic V, Skaro-Milik A, Mircic A, Djuricic B. Apoptosis induced by microtubule disrupting drugs in normal murine thymocytes *in vitro*. *Scan Microsc* 1995; **9**: 509-16.
14. Bonfoco E, Ceccatelli S, Manzo L, Nicotera P. Colchicine induces apoptosis in cerebellar granule cells. *Exp Cell Res* 1995; **218**: 189-200.
15. Lindenboim L, Haviv R, Stein R. Inhibition of drug induced apoptosis by survival factors in PC12 cells. *J Neurochem* 1995; **64**: 1054-63.
16. Nakagawa-Yagi Y. Induction of apoptotic cell death in differentiating neuroblastoma SH-SY5Y cells by colchicine. *Biochem Biophy Res Commun* 1994; **199**: 807-17.
17. Tsukidate K, Yamamoto K, Snyder JW, Farber JL. Microtubule antagonists activate programmed cell death in cultured rat hepatocytes. *Am J Pathol* 1993; **143**: 918-25.
18. Takano Y, Okudaira M, Harmon BV. Apoptosis induced by microtubule disrupting drugs in cultured human lymphoma cells. *Pathol Res Pract* 1993; **189**: 197-203.

(Receivd 30 March 1999; accepted 2 June 1999)